cell resistance to camptothecin-based anticancer drugs, such as topotecan and 7-ethyl-10-hydroxycamptothecin (SN-38: active metabolite of irinotecan). SN-38-selected PC-6/SN2-5H human lung carcinoma cells were shown to overexpress ABCG2 with a reduced intracellular accumulation of SN-38 and its glucuronide metabolite.[19] We have recently demonstrated that plasma membrane vesicles prepared from those cells transported both SN-38 and SN-38-glucuronide in an ATP-dependent manner, and our results strongly suggested that ABCG2 is involved in the active extrusion of SN-38 and its metabolite from cancer cells.[20] It remains to be elucidated, however, whether ABCG2 operates as a homodimer or a heterodimer with some other partner subunit(s).[5,9] To examine the potential role of ABCG2 as a drug transporter, we have cloned the cDNA of ABCG2 from PC-6/SN2-5H human lung carcinoma cells and characterized its function by expressing it in Sf9 insect cells.

Methods

SN-38-resistant cell line: SN-38-selected PC-6/SN2-5H human lung carcinoma cells were maintained in RPMI 1640 medium (Invitrogen Co., Carlsbad, CA, USA) supplemented with 10% fetal bovine serum (Invitrogen), 0.3 mg/ml glutamine, 0.1 mg/ml Kanamycin (Meiji Seika Co., Tokyo, Japan), and 25 nM SN-38 at 37°C in 5% CO_2 in a humidified incubator.

Cloning of human ABCG2 cDNA and generation of recombinant baculoviruses: Total RNA was extracted from PC-6/SN2-5H human lung carcinoma cells by using the ISOGEN RNA extraction kit (Nippon Gene, Tokyo, Japan). Human ABCG2 cDNA was cloned from the RNA preparation by RT-PCR with the SuperScript First-Strand Synthesis System (Invitrogen) and the following specific primers: sense 5′-CTCTCCAGATGTCTTCCAGT-3′ and antisense 5′-ACAGTGTGATGGCAAGGGAAC-3′, where the primers were designed based on the ABCG2 cDNA sequence registered in the GenBank (accession number AF098951; ref. 9). The PCR reaction consisted of 30 cycles of 95°C for 30 sec, 58°C for 30 sec, and 72°C for 2 min. The resulting PCR product was inserted into the pCR2.1 TOPO vector (Invitrogen), and its sequence was analyzed by automated DNA sequencing (TOYOBO Gene Analysis, Tokyo, Japan).

ABCG2 cDNA (Arg 482) thus obtained was removed from the pCR2.1 TOPO vector by *Eco*RI digestion. After treatment with alkaline phosphatase, ABCG2 cDNA was ligated to the *Eco*RI site of the pFASTBAC1 Expression vector (Invitrogen) by using the Rapid DNA ligation kit (Roche Diagnosis Co., Indianapolis, IN, USA). Recombinant baculoviruses with human ABCG2 cDNA were generated with the BAC-TO-BAC Baculovirus Expression Systems (Invitrogen) according to the manufacturer's instruction.

Expression of the human ABCG2 cDNA in Sf9 cells and preparation of cell membranes: Insect Spodoptera frugiperda Sf9 cells (1×10^6 cell/ml) were infected with the recombinant baculoviruses and cultured in EX-CELL™ 420 Insect serum-free medium (JRH Bioscience, Levexa, KS, USA) at 26°C with gentle shaking. Cells were harvested 48 hours after the infection by centrifugation. Subsequently, the cells were suspended in a hypotonic buffer solution containing 0.5 mM sodium phosphate (pH 7.0) and 0.1 mM EGTA and then incubated on ice for 30 min with brief ultra-sonic treatments. The resulting cell lysate mixture was centrifuged at 100,000× *g* at 4°C for 30 min. The precipitate was re-suspended in 10 mM Tris-HCl buffer (pH 7.5) and overlaid onto a 42% sucrose solution containing 10 mM Tris-HCl buffer (pH 7.5). The sample was then centrifuged in a swing rotor (Hitachi RP55S) at 100,000× *g* at 4°C for 30 min. The precipitate was collected and suspended in small volumes of 10 mM Tris-HCl buffer (pH 7.5). Protein concentrations in the membrane preparations were determined by using a BCA Protein Kit (Pierce, Rockford, IL,USA).

ATPase activity measurement: The ATPase activity of the isolated Sf9 cell membranes was determined by measuring inorganic phosphate liberation[21] according to the procedure reported by Sarkadi *et al.*[22] with some modifications. To adapt it to our high throughput screening system with 96-well plates, we developed the following standard procedure. The Sf9 cell membranes (2 μg of protein) were suspended in 10 μl of the incubation medium containing 50 mM Tris-Mes (pH 6.8), 2 mM EGTA, 2 mM dithiothreitol, 50 mM potassium chloride, 5 mM sodium azide, and 2 mM ouabain. This medium was mixed with 10 μl of a test compound solution and 10 μl of sodium vanadate solution (0–1.2 mM) and then pre-incubated at 37°C for 3 min. The ATPase reaction was started by adding 10 μl of 4 mM ATP solution to the reaction mixture (30 μl), and the incubation was maintained at 37°C for 30 min. The reaction was stopped by the addition of 20 μl of 5% trichloroacetic acid, and liberated inorganic phosphate was measured at a wavelength of 630 nm[21] in a Multiskan JX system (Dainippon Pharmaceuticals Co., Osaka, Japan).

Gel electrophoresis and detection of ABCG2 protein: Expression of ABCG2 in Sf9 cell membranes was determined by immunoblotting with BXP-21, an antibody specific to human ABCG2 (SIGNET, Dedham, MA, USA). Briefly, proteins of isolated Sf9 membranes were separated by electrophoresis on 7.5% sodium dodecyl sulfate (SDS) polyacrylamide slab gels,[23] and the proteins were electroblotted onto PVDF membranes. Immunoblotting was performed by using BXP-21 IgG as the first antibody and an anti-mouse IgG-horseradish peroxidase (HRP)-conjugate (Kirkegaad & Lerry Lab, Inc., Guthersburg, MD, USA) as the secondary an-

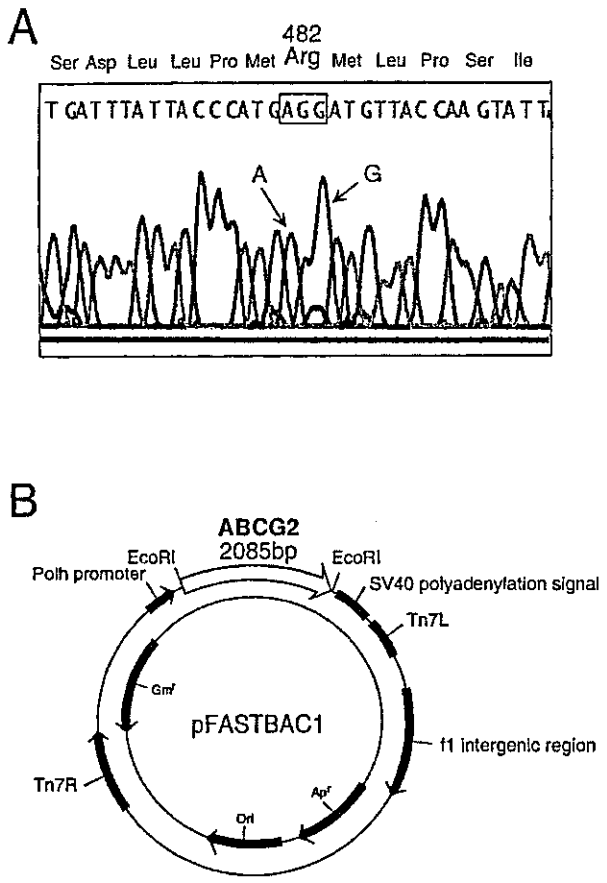

Fig. 1. cDNA of the cloned ABCG2 and its expression vector. **A**: Partial sequence of ABCG2 cDNA isolated from SN-38-selected PC-6/SN2-5H human lung carcinoma cells. The sequence demonstrates that ABCG2 expressed in the cells has arginine (Arg) at amino acid position 482. **B**: Schematic illustration of the recombinant expression vector pFASTBAC1 with the ABCG2 cDNA insert. ABCG2 cDNA was ligated to the *Eco*RI site of the pFASTBAC1 vector.

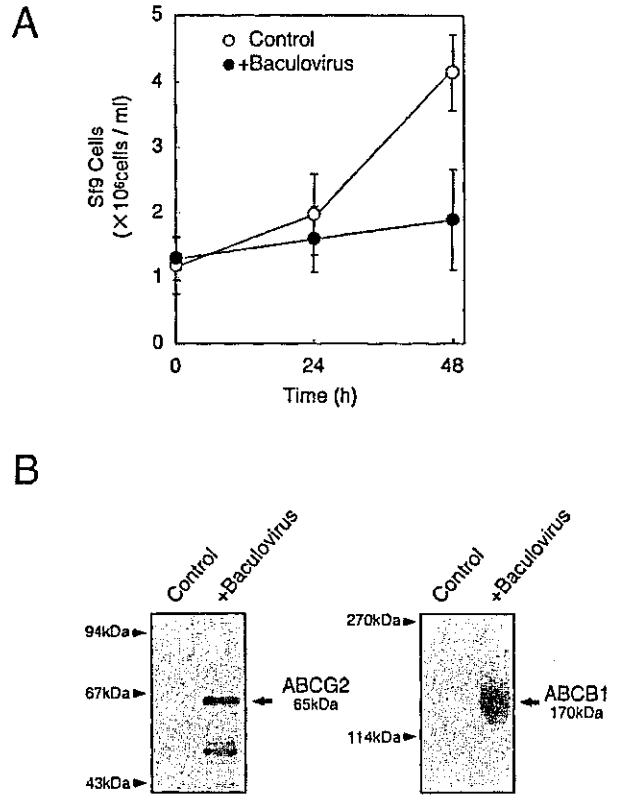

Fig. 2. Expression of ABCG2 cDNA in Sf9 cells. **A**: Growth curves of Sf9 cells uninfected (open circle) and infected with recombinant baculoviruses carrying ABCG2 cDNA (closed circle). Results are expressed as mean ± SD, n = 3. **B**: Immunoblotting detection of ABCG2 (left) and ABCB1 (right) expressed in Sf9 cell membranes.

tibody. HRP-dependent luminescence was developed by using an enhanced chemiluminescence ECL Kit (Amersham, Buckinghamshire, UK) and exposed to BIOMAX™ films (Kodak, Tokyo, Japan).

Results and Discussion

Cloning ABCG2 and its expression in Sf9 cells: In this study, we have cloned ABCG2 cDNA from the PC-6/SN2-5H human lung carcinoma cell line, which exhibited a drug resistance phenotype against SN-38 as well as high ABCG2 expression levels.[19,20] Sequence analysis has revealed that the cloned ABCG2 has an arginine at the amino acid position 482 (**Fig. 1A**). This finding is consistent with the results hitherto reported by Allikmets *et al.*[10] for ABCG2 in human placenta, as well as by Komatani *et al.*[18]

The cloned ABCG2 cDNA was expressed in Sf9 cells by means of the pFASTBAC1 vector (**Fig. 1B**) and recombinant baculoviruses. **Fig. 2A** shows the time course of Sf9 cell growth after infection with the ABCG2 cDNA-recombinant baculoviruses. The growth rate of the virus-infected cells was significantly lower than that of uninfected control cells. At 48 hours after virus infection, the cells were harvested and cell membranes were prepared. As shown in **Fig. 2B**, the expression of ABCG2 was clearly detected by immunoblotting with the BXP-21 antibody. In a separate experiment, we have cloned cDNA of ABCB1 (P-glycoprotein or MDR1) from the human liver cDNA library and expressed it in Sf9 cells by using the pFASTBAC1 vector and recombinant baculoviruses in the same manner as was carried out for ABCG2 expression (G. Wang, H. Yabuuchi, S. Tarui and T. Ishikawa, unpublished work). The ABCB1 protein, as the positive control, was detected in Sf9 cell membranes with the C219 monoclonal antibody (**Fig. 2B**).

ATPase activity in ABCG2- and ABCB1-expressing cell membranes: By using membranes prepared from Sf9 cells expressing ABCG2 and ABCB1, we have measured ATPase activity in the presence of various compounds, i.e., verapamil, SN-38, and rhodamine 123. As demonstrated in **Fig. 3B**, verapamil, one of the typical substrates of ABCB1, enhanced ATPase activity, whereas

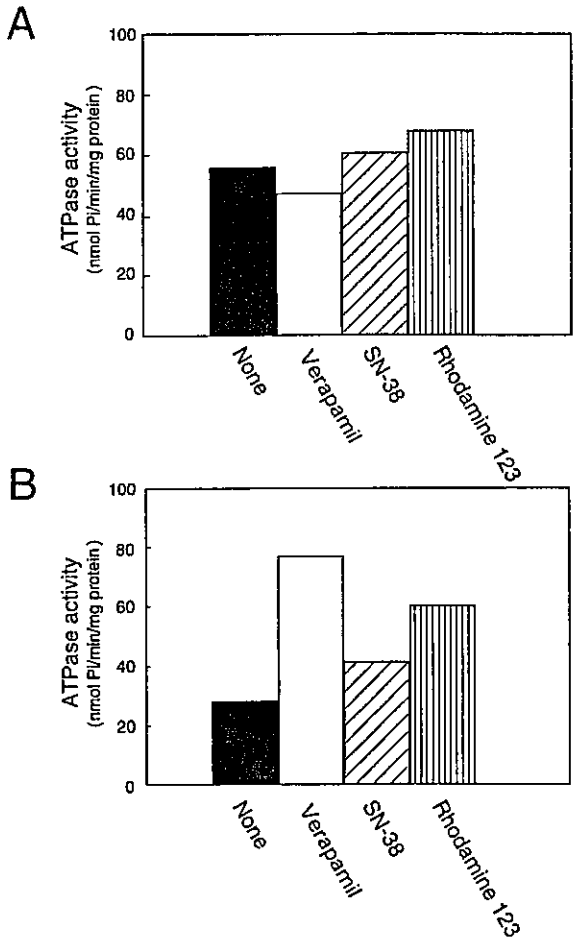

Fig. 3. Effect of verapamil, SN-38, and rhodamine 123 on the ATPase activity of cell membranes prepared from Sf9 cells. The cells were infected with recombinant baculoviruses carrying cDNA of ABCG2 (A) or ABCB1 (B). The ATPase activity was measured as described in the Methods section. Verapamil, SN-38, and rhodamine 123 were added to the reaction mixture at the final concentration of 20 μM. Results are expressed as mean values of triplicate measurements.

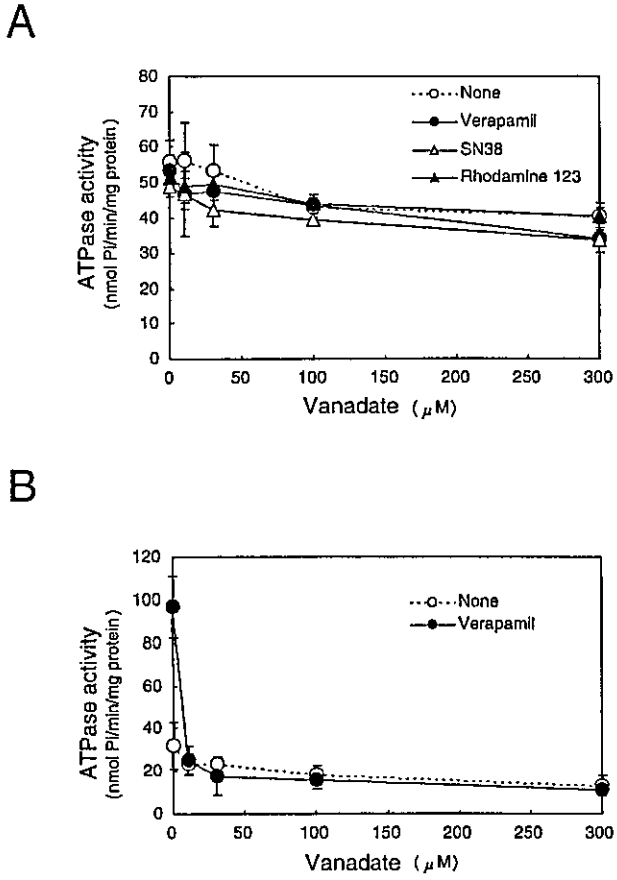

Fig. 4. Effect of vanadate on the ATPase activity of cell membranes prepared from Sf9 cells. The cells were infected with recombinant baculoviruses carrying cDNA of ABCG2 (A) or ABCB1 (B). The ATPase activity was measured as described in the Methods section. Verapamil, SN-38, and rhodamine 123 were added to the reaction mixture at the final concentration of 20 μM. The concentrations of sodium vanadate in the reaction mixture were 0, 10, 30, 100, and 300 μM as indicated in the figure. Results are expressed as mean + SD of triplicate measurements.

SN-38 was without effect. Rhodamine 123 moderately stimulated ATPase activity in the ABCB1-expressing membranes. It was, however, puzzling and also interesting that none of these compounds stimulated the ATPase activity in ABCG2-expressing cell membranes (**Fig. 3A**), although SN-38 and rhodamine 123 were originally thought to be substrates of ABCG2.[20,25] Verapamil is reportedly not a substrate of ABCG2.[24] Even in the presence of SN-38 and rhodamine 123, ATPase activity in the ABCG2-expressing cell membranes was little affected by sodium vanadate (up to 300 μM) (**Fig. 4A**). By contrast, in the ABCB1-expressing cell membranes, verapamil-stimulated ATPase activity was very sensitive to vanadate (**Fig. 4B**), where ATPase activity was almost completely inhibited to background levels by 100 μM sodium vanadate.

Variants of ABCG2 and their substrate specificities: Recently, at least three variant forms of ABCG2 have been recognized on the basis of the amino acid moieties identified at position 482 close to the third transmembrane domain. The wild-type ABCG2 has an arginine at that position,[10] whereas other variants cloned from cancer cell lines, such as MCF-7/AdVp cells[9] and S1-M1-80 cells,[13] have threonine and glycine at position 482, respectively. It is currently speculated that the substrate specificity of ABCG2 may differ among those variant forms.[18,25] In fact, transfectants with the wild type (Arg 482) were not resistant to mitoxantrone or topotecan,[18] whereas overexpression of Thr 482 and Gly 482 variants conferred resistance to mitoxantrone, doxorubicin, daunorubicin, and various camptothecin analogs including topotecan.[9,14-16] Furthermore, the Thr 482 and Gly 482 variants mediated the respective efflux of rhodamine 123 and doxorubicin from cells, however, the wild type (Arg 482) did not.[25]

It is important to note that the ABCG2 cloned in this study has an arginine at the amino acid position 482, as does the wild type. Therefore, it is considered reasonable that the ATPase activity of cell membranes expressing our cloned ABCG2 was not stimulated by rhodamine 123. This finding, of course, does differ from the recent study of Özvegy *et al.*[24] in which the Gly 482 variant was expressed in Sf9 cells for the ATPase activity assay. In this context, it is of importance to carefully elucidate which type of variant was used to analyze the substrate specificity of ABCG2. In addition, based on the apparent discrepancy demonstrated in this study, genetic polymorphism of ABCG2 is suggested to be a critical factor affecting the substrate specificity.[26]

It is known that the *Drosophila white* gene product, a homolog of ABCG2, forms a heterodimer with one of its homologs, *brown or scarlet*, and that the different dimers transport different eye pigment precursor molecules.[27] Therefore, human ABCG2 is also suggested to form a heterodimer by recruiting a partner protein(s) whereby ABCG2 can exhibit a broad spectrum of substrate specificity. As shown in the present study, ATPase activity in the cell membranes expressing our cloned ABCG2 was not significantly stimulated by SN-38 (**Fig. 4A**), even though ABCG2 was cloned from drug resistant cancer cells in which SN-38 accumulation was substantially reduced.[19,20] On the other hand, HEK293 cells transfected with our ABCG2 cDNA exhibited 13- to 20-fold resistance to SN-38, as compared with the untransfected control HEK293 cells (Yoshikawa *et al.*, unpublished data). Thus, our data suggest that there is a partner protein of ABCG2 required for heterodimer formation.

ABCG2 belongs to the G subfamily of human ABC transporters. In this subfamily, ABCG1, ABCG5, and ABCG8 have already been shown to be critically involved in the regulation of lipid- and sterol-trafficking mechanisms in macrophages, hepatocytes, and intestinal mucosa cells.[28-30] ABCG2 is expressed not only in cancer cells, but also endogenously in placental syncytiotrophoblasts, the epithelium of the small intestine and liver canalicular membrane, as well as in ducts and lobules of the breast.[31] The apical localization in the epithelium of the small intestine and colon indicates a possible role of ABCG2 regulating the uptake of p.o. administered drugs. Furthermore, it has most recently been reported that ABCG2 is expressed in a wide variety of stem cells, and its potential role in the regulation of hematopoietic development is suggested.[32] To date, however, endogenous substrates of ABCG2 in stem cells have not been identified. Further studies are needed to facilitate our understanding of the nature and biological function of the human ABCG2 protein.

Acknowledgments: SN-38 was kindly provided by Yakult Honsha Co. (Tokyo, Japan).

This study was supported by a research grant (H12-Genome-026) entitled "Studies on the genetic polymorphism and function of pharmacokinetics-related proteins in Japanese population" from the Japanese Ministry of Health and Welfare as well as, in part, by research grants of a NEDO project "Development of the hepatocyte-chip for drug toxicity evaluation" and Grant-in-Aid for Creative Scientific Research (No. 13NP0401) of Japan Society for the Promotion of Science.

References

1) Ling, V.: Multidrug resistance: molecular mechanisms and clinical relevance. *Cancer Chemother. Pharmacol.*, **40**: S3-S8 (1997).
2) Ambudkar, S. V., Dey, S., Hrycyna, C. A., Ramachandra, M., Pastan, I. and Gottesman, M. M.: Biochemical, cellular, and pharmacological aspects of the multidrug transporter. *Annu. Rev. Pharmacol. Toxicol.*, **39**: 361-398 (1999).
3) Borst, P., Evers, R., Kool, M. and Wijnholds, J.: The multidrug resistance protein family. *Biochim. Biophys. Acta*, **1461**: 347-357 (1999).
4) Ishikawa, T., Kuo, M. T., Furuta, K. and Suzuki, M.: The human multidrug resistance-associated protein (MRP) gene family: from biological function to drug molecular design. *Clin. Chem. Lab. Med.*, **38**: 893-897 (2000).
5) Klein, I., Sarkadi, B. and Váradi, A.: An inventory of the human ABC proteins. *Biochim. Biophys. Acta*, **1461**: 237-262 (1999).
6) Ishikawa, T., Allikmets, R., Dean, M., Higgins, C., Ling, V. and Wain, H. M.: New nomenclature of human ABC transporter genes. *Xenobio. Metabol. Dispos.*, **15**: 8-19 (2000).
7) Dean, M., Rzhetsky, A. and Allikmets, R.: The human ATP-binding cassette (ABC) transporter superfamily. *Genome Res.*, **11**: 1156-1166 (2001).
8) Higgins, C. F.: ABC transporters: from microorganisms to man. *Annu. Rev. Cell Biol.*, **8**: 67-113 (1992).
9) Doyle, L. A., Yang, W., Abruzzo, L. V., Krogmann, T., Gao, Y., Rishi, A. K. and Ross, D. D.: A multidrug resistance transporter from human MCF-7 breast cancer cells. *Proc. Natl. Acad. Sci. USA*, **95**: 15665-15670 (1998).
10) Allikmets, R., Schriml, L. M., Hutchinson, A., Romano-Spica, V. and Dean, M.: A human placenta-specific ATP-binding cassette gene (ABCP) on chromosome 4q22 that is involved in multidrug resistance. *Cancer Res.*, **58**: 5337-5339 (1998).
11) Hazlehurst, L. A., Foley, N. E., Gleason-Guzman, M. C., Hacker, M. P., Cress, A. E., Greenberger, L. W., de Jong, M. C. and Dalton, W. S.: Multiple mechanisms confer drug resistance to mitoxantrone in the human 8226 myeloma cell line. *Cancer Res.*, **59**: 1021-1028 (1998).
12) Rabindran, S. K., He, H., Singh, M., Brown, E.,

Collins, K. I., Annable, T. and Greenberger, L. M.: Reversal of a novel multidrug resistance mechanism in human colon carcinoma cells by fumitremorgin C. *Cancer Res.*, **58**: 5850–5858 (1998).

13) Miyake, K., Mickley, L., Litman, T., Zhan, Z., Robey, R., Cristensen, B., Brangi, M., Greenberger, L., Dean, M., Fojo, T. and Bates, S. E.: Molecular cloning of cDNAs which are highly overexpressed in mitoxantrone-resistant cells: demonstration of homology to ABC transport genes. *Cancer Res.*, **59**: 8–13 (1999).
14) Maliepaard, M., van Gastelen, M. A., de Jong, L. A., Pluim, D., van Waardenburg, R. C. A. M., Ruevekamp-Helmers, M. C., Floot, B. G. J. and Schellens, J. H. M.: Overexpression of the BCRP/MXR/ABCP gene in a topotecan-selected ovarian tumor cell line. *Cancer Res.*, **59**: 4559–4563 (1999).
15) Ross, D. D., Yang, W., Abruzzo, L. V., Dalton, W. S., Schneider, E., Lage, H., Dietel, M., Greenberger, L., Cole, S. P. C. and Doyle, L. A.: Atypical multidrug resistance: breast cancer resistance protein messenger RNA expression in mitoxantrone-selected cell lines. *J. Natl. Cancer Inst.*, **91**: 429–433 (1999).
16) Brangi, M., Litman, T., Ciotti, M., Nishiyama, K., Kohlhagen, G., Takimoto, C., Robey, R., Pommier, Y., Fojo, T. and Bates, S. E.: Camptothecin resistance: role of the ATP-binding cassette (ABC), mitoxantrone-resistance half-transporter (MXR), and potential for glucuronidation in MXR-expressing cells. *Cancer Res.*, **59**: 5938–5946 (1999).
17) Litman, T., Brangi, M., Hudson, E., Fetsch, P., Abati, A., Ross, D. D., Miyake, K., Resau, J. H. and Bates, S. E.: The multidrug-resistant phenotype associated with overexpression of the new ABC half-transporter, MXR (ABCG2). *J. Cell Sci.*, **113**: 2011–2021 (2000).
18) Komatani, H., Kotani, H., Hara, Y., Nakagawa, R., Matsumoto, M., Arakawa, H. and Nishimura, S.: Identification of breast cancer resistant protein/mitoxantrone resistance/placenta-specific, ATP-binding cassette transporter as a transporter of NB-506 and J-107088, topoisomerase I inhibitors with an indolocarbazole structure. *Cancer Res.*, **61**: 2827–2832 (2001).
19) Kawabata, S., Oka, M., Shiozawa, K., Tsukamoto, K., Nakatomi, K., Soda, H., Fukuda, M., Ikegami, Y., Sugahara, K., Yamada, Y., Kamihara, S., Doyle, L. A., Ross, D. D. and Kohno, S.: Breast cancer resistance protein directly confers SN-38 resistance of lung cancer cells. *Biochem. Biophys. Res. Commun.*, **280**: 1216–1223 (2001).
20) Nakatomi, K., Yoshikawa, M., Oka, M., Ikegami, Y., Hayasaka, S., Sano, K., Shiozawa, K., Kawabata, S., Soda, H., Ishikawa, T., Tanabe, S. and Kohno, S.: Transport of 7-ethyl-10-hydroxycamptothecin (SN-38) by breast cancer resistance protein ABCG2 in human lung cancer cells. *Biochem. Biophys. Res. Commun.*, **288**: 824–832 (2001).
21) Carter, S. G. and Karl, D. W.: Inorganic phosphate assay with malachite green: an improvement and evaluation. *J. Biochem. Biophys. Methods*, **7**: 7–13 (1982).
22) Sarkadi, B., Price, E. M., Boucher, R. C., Germann, U. A. and Scarborough, G. A.: Expression of the human multidrug resistance cDNA in insect cells generates a high activity drug-stimulated membrane ATPase. *J. Biol. Chem.*, **267**: 4854–4858 (1992).
23) Laemmli, U. K.: Cleavage of structural proteins during the assembly of the head of bacteriophage T4. *Nature*, **227**: 680–685 (1970).
24) Özvegy, C., Litman, T., Szakács, G., Nagy, Z., Bates, S., Váradi, A. and Sarkadi, B.: Functional characterization of the human multidrug transporter, ABCG2, expressed in insect cells. *Biochem. Biophys. Res. Commun.*, **285**: 111–117 (2001).
25) Honjo, Y., Hrycyna, C. A., Yan, Q.-W., Medina-Párez, W. Y., Robey, R. W., van de Laar, A., Litman, T., Dean, M. and Bates, S. E.: Acquired mutations in the *MXR/BCRP/ABCP* gene alter substrate specificity in *MXR/BCRP/ABCP*-overexpressing cells. *Cancer Res.*, **61**: 6635–6639 (2001).
26) Ishikawa, T., Yabuuchi, H., Kasamatsu, S., Yoshikawa, M. and Ikegami, Y.: Pharmacogenomics in drug discovery and development research. *Xenobio. Metabol. Dispos.*, **16**: 353–363 (2001).
27) Dreesen, T. D., Johnson, D. H. and Henikoff, S.: The brown protein of Drosophila melanogaster is similar to the white protein and to components of active transport complexes. *Mol. Cell. Biol.*, **8**: 5206–5215 (1988).
28) Schmitz, G., Langmann, T. and Heimerl, S.: Role of ABCG1 and other ABCG family members in lipid metabolism. *J. Lipid Res.*, **42**: 1513–1520 (2001).
29) Klucken, J., Buchler, C., Orso, E., Kaminski, W. E., Porsch-Ozcurumrz, M., Liebisch, G., Kapinsky, M., Diederich, W., Drobnik, W., Dean, M. and Allikmets, R.: ABCG1 (ABC8), the human homolog of the *Drosophila white* gene, is a regulator of macrophage cholesterol and phospholipid transport. *Proc. Natl. Acad. Sci.*, **97**: 817–822 (2000).
30) Berge, K. E., Tian, H., Graf, G. A., Yu, L., Grishin, N. V., Schultz, J., Kwiterovich, P., Shan, B., Barnes, R. and Hobbs, H. H.: Accumulation of dietary cholesterol in sitosterolemia caused by mutations in adjacent ABC transporters. *Science*, **290**: 1771–1775 (2000).
31) Maliepaard, M., Scheffer, G. L., Faneyte, I. F., van Gastelen, M. A., Pijnenborg, A. C. L. M., Schinkel, A. H., van de Vijver, M. J., Scheper, R. J. and Schellens, J. H. M.: Subcellular localization and distribution of the breast cancer resistance protein transporter in normal human tissues. *Cancer Res.*, **61**: 3458–3464 (2001).
32) Zhou, S., Schuetz, J. D., Bunting, K. D., Colapietro, A.-M., Sampath, J., Morris, J. J., Lagutina, I., Grosveld, G. C., Osawa, M., Nakauchi, H. and Sorrentino, B. P.: The ABC transporter Bcrp1/ABCG2 is expressed in a wide variety of stem cells and is a molecular determinant of the side-population phenotype. *Nature Med.*, **7**: 1028–1034 (2001).

SERUM- AND SERUM DEPRIVATION-INDUCED TRANSCRIPTIONAL PROFILES OF CULTURED CONJUNCTIVAL EPITHELIAL CELLS

Akihiro Higuchi,[1] Shigeto Shimmura,[1] Masami Ishii,[2]
Hiroyuki Aburatani,[2] and Kazuo Tsubota[1]

[1]Department of Ophthalmology

Tokyo Dental College
Chiba, Japan
[2]Research Center for Advanced Science and Technology
The University of Tokyo
Tokyo, Japan

1. INTRODUCTION

Severe dry eye is caused not only by the dryness of the ocular surface, but also by lack of tear components, which are essential to maintain the ocular surface.[1] Artificial tears are useful as a therapy for dry eye, but the efficiency of artificial tears is not comparable to human tears. We have used autologous serum as a substitute for tears in severe dry eye patients, and have observed dramatic improvements to the ocular surface.[2] This serum effect suggests that serum includes similar components to tears

The aim of this study is the elucidation of the mechanism by which human serum supports the survival of ocular surface cells. The conjunctival epithelial cell line, CCL-20.2 (CCL), which requires serum in the medium to survive, was used as a model system of the ocular surface. It is well known that apoptosis occurs when the culture medium of some cells, including CCL, is deprived of serum or growth factors. It has been suggested that myc[3] and p53 play roles in this apoptosis, however, the precise mechanism is not known. We investigated temporal changes in the mRNA levels of approximately 5,600 human genes using the GeneChip microarray to elucidate the effects of serum deprivation and serum stimulation on cultured CCL.[4]

Lacrimal Gland, Tear Film, and Dry Eye Syndromes 3
Edited by D. Sullivan *et al.*, Kluwer Academic/Plenum Publishers, 2002

2. MATERIALS AND METHODS

2.1. Cell Culture

CCL at passage 10 were grown to about 70% confluence in 75 cm^2 flasks in Medium 199 (Gibco BRL Life Technologies, Rockville, MD) containing 20% human serum. Cells were harvested from several flasks to isolate mRNA prior to serum deprivation. This mRNA served as non-deprivation control. The remaining cells were then washed with PBS, and the medium was changed to Medium 199 containing 0.1% human serum. After 24 h, cells were harvested from several flasks to isolate mRNA. These served as deprivation or time-zero control. The medium of other flasks was replaced with Medium 199 containing 20% human serum. After re-addition of Medium 199 with 20% human serum, cells were harvested from several flasks at 3 time points, 30 min, 6 and 24 h. The harvested-cells were washed with PBS, and was lysed to isolate poly $(A)^+$ mRNA by QuickPrep (Amersham Pharmacia Biotech, Piscataway, NJ).

2.2. GeneChip Hybridization

The GeneChip experimental procedures were performed according to the Affymetrix GeneChip Expression Analysis Technical Manual (Affymetrix Inc, Santa Clara, CA).[5] The human GeneChip array, HuGeneFL array (Affymetrix Inc), which contains probe sets for approximately 5600 human genes, was used for hybridization. After hybridization, the GeneChip array was stained by streptavidin-phycoerythrin (Molecular Probes, Eugene, OR), amplified with biotinylated anti-streptavidin (Vector Laboratories, Inc., Burlingame, CA), and scanned using an HP GeneArray scanner according to the manufacturer's protocol.

The intensity of each feature of each array was captured using GeneChip software (version 3.0) according to standard Affymetrix procedures.[6] As described previously,[7] the change in the level of expression for any gene was considered significant when there was a 3-fold change in the intensity across the probe set.

3. RESULTS

3.1. Changes in mRNA Transcripts Induced by Serum Deprivation

Serum deprivation induced changes in CCL mRNA levels. The mRNA levels of 18 proteins increased, and there was a more than 3 fold decrease in the mRNA levels of 13 proteins. Some of the largest changes are summarized in Table 1. Notably, increases in transcripts for immediate early response 3 and jun B, components of the anti-apoptosis response system, were observed after serum deprivation.

Table 1. Changes of mRNA expression induced by serum deprivation

Description	Change	Fold
jun B	Increase	5.3
Integrin beta 4	Increase	5.2
Transcobalamin I	Increase	5.2
Immediate early response 3	Increase	4.4
20-kDa myosin light chain	Decrease	13.5
22-kDa smooth muscle protein	Decrease	7.0

3.2. Changes in mRNA Transcripts Induced by Serum Addition

Serum stimulation, following 24 h of serum deprivation, induced >3-fold increases in mRNA levels of 64 proteins, and >3-fold decreases in mRNA levels of 40 proteins in at least 1 time point. These results are summarized in Table 2.

Table 2. Changes of mRNA expression induced by serum stimulation

DescriptionTime	Time	Change	Fold
Transforming protein fos-B	0.5	Increase	17.7
Steroid hormone receptor TR3	0.5	Increase	14.3
Connective tissue growth factor	0.5	Increase	12.2
22kDa smooth muscle protein	6	Increase	11.0
RTVP-1 protein	6	Increase	7.8
Heparin-binding EGF-like growth factor	6	Increase	7.0
Selenophosphate synthetase	24	Increase	5.2
Tumor necrosis factor receptor	24	Increase	4.9
22kDa smooth muscle protein	24	Increase	4.5
Transcription regulator helix-loop-helix protein	6	Decrease	11.4
TGF-beta superfamily protein	6	Decrease	6.4
MXI1	6	Decrease	6.2
E1A enhancer-binding protein	24	Decrease	5.1
Uracil-DNA glycosylase	24	Decrease	4.3
Transcobalamin	24	Decrease	4.1

3. DISCUSSION

Since serum components are similar to tear components, symptoms of severe dry eye, caused in part by a lack of certain tear components, is improved by autologous serum therapy.[2] In this study, we used a conjunctival epithelial cell line model to investigate the mechanisms by which the ocular surface is maintained by serum components. Serum effects on CCL survival suggest that components of tears play an important role in the maintenance of ocular epithelial cells, and that the use of autologous serum as a tear replacement therapy may be effective in performing a similar role in patients with dry eye.

Serum deprivation of CCL cultures causes many changes in various protein levels in the cells. Some of these changes occurred in proteins associated with induction or prevention of apoptosis. Interestingly, the mRNA levels of apoptosis-related proteins were not changed (data not shown). This result is differs with previous studies, in which the apoptotic response depended on mRNA expression and protein synthesis.[8] However, it is possible that apoptosis-related mRNA expression has already completed after 24 h following serum deprivation, and apoptosis responses are mainly due to protein-protein reactions. Some of these proteins, such as immediate early response 3 and jun B, where mRNA levels increased after serum deprivation (Table 1), could be related to an anti-apoptosis response.[9,10] These factors should protect CCL from serum deprivation-induced cell death, either in tandem or cooperatively.

In this study, serum deprivation- and serum stimulation-induced CCL expression data for approximately 5,600 mRNAs were obtained by GeneChip. Using these data, we can elucidate the mechanisms by which CCL and ocular surface cells are maintained, and develop effective novel formulations of artificial tears.

REFERENCES

1. Y.Ohashi, M.Motokura, Y.Kinoshita, et al. Presence of epidermal growth factor in human tears. *Invest Ophthalmol Vis Sci.* 30:1879 (1989).
2. K.Tsubota, E.Goto, H.Fujita, et al. Treatment of dry eye by autologous serum application in Sjogren's syndrome. *Br J Ophthalmol.* 83:390 (1999).
3. G.Packham, C.W.Porter, J.L.Cleveland. c-Myc induces apoptosis and cell cycle progression by separable, yet overlapping, pathways. *Oncogene.* 13:461 (1996).
4. R.J.Lipshutz, S.P.Fodor, T.R.Gingeras, D.J.Lockhart. High density synthetic oligonucleotide arrays. *Nat Genet.* 21 (1 Suppl):20 (1999).
5. D.J.Lockhart, H.Dong, M.C.Byrne, et al. Expression monitoring by hybridization to high-density oligonucleotide arrays. *Nat Biotechnol* 14:1675 (1996).
6. C.K.Lee, R.G.Klopp, R.Weindruch, T.A.Prolla. Gene expression profile of aging and its retardation by caloric restriction. *Science* 285:1390 (1999).
7. H.Zhu, J.P.Cong, G.Mamtora, T.Gingeras, T.Shenk. Cellular gene expression altered by human cytomegalovirus: global monitoring with oligonucleotide arrays. *Proc Natl Acad Sci U S A.* 95:14470 (1998).
8. Y.Koyama, Y.Kimura, Y.Yoshioka, et al. Serum-deprivation induces cell death of rat cultured microglia accompanied with expression of Bax protein. *Jpn J Pharmacol.* 83:351 (2000).
9. M.X.Wu, Z.Ao, K.V.Prasad, R.Wu, S.F.Schlossman. IEX-1L, an apoptosis inhibitor involved in NF-kappaB-mediated cell survival. *Science.* 281:998 (1998).
10. J.Lotem, L.Sachs. Different mechanisms for suppression of apoptosis by cytokines and calcium mobilizing compounds. *Proc Natl Acad Sci U S A.* 95:4601 (1998).

J Gastroenterol 2002; 37[Suppl XIV]:62–66

Journal of Gastroenterology

Gene expression profile after peroxisome proliferator activator receptor-γ ligand administration in dextran sodium sulfate mice

Atsushi Nakajima[1], Koichiro Wada[2], Kazufumi Katayama[2], Lawrence Saubermann[3], Emi Osawa[1], Hajime Nagase[1], Norio Ueno[1], Nobuyuki Matsuhashi[4], and Hiroyuki Aburatani[5]

[1]Third Department of Internal Medicine, Yokohama City University School of Medicine, 3-9 Fukuura, Kanazawa-ku, Yokohama 236-0004, Japan
[2]Department of Pharmacology, Graduate School of Dentistry, Osaka University, Suita, Japan
[3]Section of Gastroenterology, Boston University Medical Center, Boston, MA, USA
[4]Department of Medicine, University of Tokyo, Tokyo, Japan
[5]Genome Science Division, Research Center for Advanced Science and Technology, The University of Tokyo, Tokyo, Japan

Background. Peroxisome proliferator activator receptor-gamma (PPARγ) is a member of the nuclear receptor superfamily. Ligands of PPARγ, thiazolidione derivatives, have been reported to be the one of the candidates for the treatment of inflammatory bowel disease (IBD). Given the fact that PPARγ is a transcription regulator, expression pharmacogenomics, including differential gene expression profiling of drug responses in a colitis model, is thought to be a useful approach for finding relevant genes that can serve as the target for new drug treatment of IBD. ***Methods.*** We performed a global analysis for differential gene expression of the intestine in a dextran sodium sulfate (DSS) colitis mouse model following PPARγ ligand administration. By applying a high-density oligonucleotide array method, the expression patterns of approximately 12000 genes were analyzed, and selected genes were confirmed by a real-time quantitative PCR method. ***Results.*** The analysis of downregulated genes in the DSS mice following PPARγ administration revealed several functional gene clusters with altered expression: (1) oncogene families such as GRO1 oncogenes, (2) inflammatory mediator-related genes such as the interferon-gamma gene, (3) water electrolyte-associated genes, and (4) others. ***Conclusions.*** This is the first demonstration of global gene expression analysis using the DSS colitis mouse model with a PPARγ ligand, and these results provide new insight for finding novel target genes for treating IBD.

Key words: peroxisome proliferator activator receptor-gamma (PPARγ), gene profiling, oligonucleotide microarray, dextran sodium sulfate (DSS) colitis mouse model

Reprint requests to: A. Nakajima

Introduction

Although the pathogenesis of in flammatory bowel disease (IBD) remains to be elucidated, various kinds of inflammatory cytokines and adhesion molecules have been reported to play a pivotal role in the IBD disease process. For example, tumor necrosis tactor-alpha (TNF-α) correlates with the progression of Crohn's disease, and an antibody specific for TNF-α is used to treat Crohn's disease.[1]

Multiple gene expressions are involved in the onset and progression of IBD; however, too many genes are involved on the inflammatory locus to be analyzed by global gene expression analysis.[2–4] Therefore, differential gene expression profiling of drug responses in a colitis model is more appropriate to determine a set of differentially modulated drug-responsive genes.

Peroxisome proliferator-activated receptor-gamma (PPARγ) is a nuclear receptor that was originally shown to play a critical role in adipocyte differentiation and insulin sensitivity.[5–7] PPARγ is activated by several ligands, including 15-deoxy-Δ-12,14-prostaglandin J_2 and thiazolidinedione derivatives (TZDs), such as troglitazone, pioglitazone, and rosiglitazone (BRL-49653), which are used as oral antihyperglycemic agents for treating diabetes mellitus. Recently, these ligands have been reported to have therapeutic effects in mouse IBD models.[8] Considering that PPARγ is a nuclear receptor that can regulate gene expression, gene expression profiling is thought to be a very useful technique for elucidating drug action. Furthermore, these results will provide the novel genes that play an important role for the pathogenesis of IBD.

In this study, we globally analyzed the expression profiles of approximately 12000 genes in the dextran sodium sulfate (DSS) colitis model related to PPARγ by using a high-density oligonucleotide array.[9] By combining this analysis with subsequent confirmation of altered expression in selected genes by quantitative RT-PCR,

we identified differently expressed genes. Although further functional analysis is necessary, these results provide new insight on the pathological mechanisms of IBD.

Materials and methods

Mice

Inbred C57BL/6 mice were purchased from CLEA Japan (Tokyo, Japan). All animals were maintained under specific pathogen-free conditions on standard laboratory diets and water ad libitum, until the desired age (7–10 weeks) and weight (20–30 g) were achieved. All mice were treated humanely according to the guidelines of NIH, IACUC, and the Panel on Euthanasia of the American Veterinary Medical Association'.

Dextran sodium sulfate (DSS) colitis model

All mice were treated humanely according to the National Institutes of Health and AERI-BBRI Animal Care and Use Committee guidelines. All animal experiments were approved by the institutional animal care and use committee of Yokohama City University School of Medicine.

Specific pathogen-free, male C57BL/6J mice were purchased from CLEA Japan (Tokyo, Japan). Colitis was induced in 8-week-old mice (weighing 20–25 g) using 2.5% (w/v) DSS in the drinking water, which caused clinical symptoms of IBD within 7 days.[10] To investigate the therapeutic effects of the PPARγ ligand, BRL-49653, in DSS-induced colitis, we prepared two groups 4 days after inducing colitis: a group pretreated with BRL-49653 (10 mg/kg) and an untreated group. In this protocol for the intervention studies, DSS was administered on day 0 and was continued until day 4, at which time the animals were killed. The PPARγ ligand, BRL-49653, was suspended in distilled water and administered orally (30 mg/kg/day) from day 0 to day 4.

Reagents

Rosiglitazone (BRL-49653) was generously donated by SmithKline-Beecham (Tokyo, Japan). Other reagents were of chemical grade.

High-density oligonucleotide array analysis

Total RNA was isolated from the colon of the DSS mouse on day 1 and day 4 using Isogen RNA isolation reagent (Nippon Gene, Toyama, Japan). From the colon of each DSS mouse, 1 μg polyadenylated RNA was amplified up to approximately 100 μg cRNA using T7-based amplification and hybridized to the high-density oligonucleotide array (GeneChip; U74, Affymetrix, Santa Clara, CA, USA) as described previously.[11] Three samples from each group were analyzed. The intensity for each future array was calculated by using Affymetrix GeneChip version 3.3 software with a class ABC mask file. This so-called mask file is designed to exclude inappropriate probe pairs and probe sets that represent introns or reverse sequences. The average intensity was made equal to the target intensity, which was set to 100, to reliably compare variable multiple arrays. In calculating the changes of average difference, normalization for all probe sets was performed. A dot-plot analysis of the fold change in the gene expression patterns was performed by the same software.

Real-time quantitative RT-PCR

Quantitative PCR was performed for the validation of the result of array analysis using cDNA samples derived through reverse transcription-PCR of whole colon mRNA as previously described.[12] mRNA was isolated using the RNAeasy kit (Qiagen, Hilden, Germany), and then the RT-PCR procedure was performed using MMLV reverse transcriptase as previously described. The cDNA amounts and purity were checked by spectophotometer using the DU-640 spectophotometer at wavelengths 260 and 280. The cDNA samples were then used as templates for individual PCR reactions using specific primer sets, which were designed by the Primer Express software (Applied Biosystems, Urayasu, Japan). PCR reactions were prepared using a SYBR Green PCR kit (Applied Biosystems). The quantitative PCR analysis was performed using an ABI 7700 realtime PCR machine (TaqMan).[12]

Results

Global gene expression analysis of the DSS colitis mouse by high-density oligonucleotide array

We first performed a global analysis of gene expression patterns of 12000 genes in DSS colitis mice at day 4 using high-density oligonucleotide arrays and compared the gene expression profiles to the patterns noted with PPARγ ligand.

As shown in Fig. 1, a dot-plot analysis of the fold change in the gene expression patterns in DSS colitis treated with the PPARγ ligand, BRL-49653, compared to DSS colitis alone showed many expressed differently in the tissue with and without associated PPARγ. The genes plotted on the diagonal line are the genes expressed equivalently, and the genes plotted far from the diagonal line are the genes expressed differently (see Fig. 1).

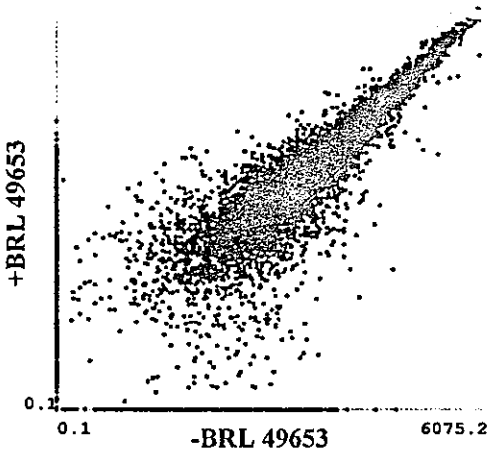

Fig. 1. Plot comparing hybridization intensities for individual genes from the intestinal specimen of the dextran sodium sulfate (DSS) colitis mouse and the specimen of DSS colitis mouse treated with PPARγ ligand on day 4. *Inner solid and outer dashed lines* indicate expression difference of threefold and tenfold, respectively

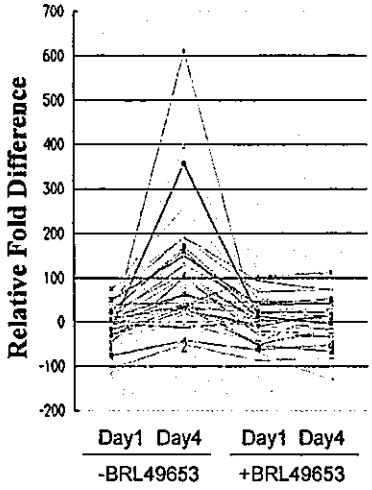

Fig. 2. Gene clustering sorted according to condition, in which genes increased in DSS colitis and decreased in DSS colitis treated with PPARγ on day 4. Individual genes are listed in Table 1

Table 1. Genes upregulated in dextran sodium sulfate (DSS) colitis and downregulated in DSS colitis associated to peroxisome proliferator-activated receptor-gamme (PPARγ)

GenBank	Sort score	qRT-PCR	Gene
D63362	−45.39	−70	Mouse DNA for regIII gamma protein
M96827	−41.3	−72	Haptoglobin
M16360	−40.94	−80	Major urinary protein 5
X66402	−40.42	−56	Matrix metalloproteinase 3
D63359	−40.37	−50	Pancreatic-associated protein
X99347	−33.67	−52	Lipopolysaccharide-binding protein
X66473	−33.48	−48	Matrix metalloproteinase 13
X04653	−32.68	−40	Ly-6 alloantigen
AJ007971	−32.38	−44	Interferon-inducible GTPase
J04596	−12.27	−46	GRO1 oncogene
AI836812	−12.11	−30	RAB5C, member RAS oncogene family
U73487	−11.89	−30	Calcium channel, voltage-dependent, alpha2/delta subunit 1
D42124	−11.75	−22	V-maf
U20735	−11.71	−26	*Jun-B* oncogene
U43085	−11.69	−30	Interferon-induced protein with tetratricopeptide
AFO49850	−11.59	−30	Major histocompatibility complex (MHC) III
X52643	−11.45	−26	Histocompatibility class II antigen A
X56602	−11.42	−25	Interferon-inducible protein
U88623	−11.42	−32	Aquaporin 4
U28405	−11.40	−35	Chemokine (C-C) receptor 1
Y13185	−11.39	−24	Matrix metalloproteinase 10
XM125899	−11.0	−23	Interferon gamma

Sort score, difference in gene expression change; qRT-PCR, quantitative RT-PCR

Genes expressed differently in the DSS colitis mouse associated with PPARγ

As shown in Fig. 2, we next sorted the genes according to the condition in which the genes increased in DSS colitis and decreased in DSS colitis treated with PPARγ at day 4. These genes were further sorted by the sort score and listed in Table 1.

Validation of selected genes by real-time quantitative RT-PCR

To verify the data, we then performed quantitative RT-PCR testing on a total of 50 genes. The genes concordant in both analyses are listed in Table 1; the ratio of concordance was 60%.

Table 2. Primer sets for quantitative PCR

Gene	5′-Forward	3′-Reverse
Mouse DNA for regIII gamma protein	AATCACTGATATAAATATTA	AAAATATTGCAACCTTGAGT
Haptoglobin	GGACTCACCACCGGGGCCAC	AGCTGGTTTTTCCCCACGTA
Major urinary protein 5	CCTGGCCTCTGACAAAAGAG	CCAAATATATTTCAGTGCAC
Matrix metalloproteinase 3	GGAGATGCTCACTTTGACGA	ACTGGGTACATCAGAGCTTC
Pancreatic-associated protein	CATGGTGAAGAGAACAGGAA	ACGGTCTAAGGCAGTAGATG
Lipopolysaccharide-binding protein	CCTGAACTTTTCCATCACAG	AGACCACTGTTCTAAGGAGC
Matrix metalloproteinase 13	TGCATATGAACATCCATCCC	ACACGTGGTTCTCAGAGAAG
Ly-6 alloantigen	CAATCTTTGCTTACCCATCT	CCATGGTCCAGGTGCTGCCT
Interferon-inducible GTPase	TGGAGACTCTGAAGAAAAGC	CAAACAACTCCTGAATAT
GRO1 oncogene	GAAGACAGACTGCTCTGATG	TTAAATATTAATGTAAAATA
RAB5C, member RAS oncogene family	CGATCGGCTGACTATATTGAC	TGACTCCCAGCTGGGAGAGA
Calcium channel, voltage-dependent, alpha2/delta subunit 1	TGAGCGGATTGACTCTGAA	GATCCCCTTTGCTGTAATGT
V-maf	CTGCTTGTCAGCACCGTGG	GCCTGTGTACACACAGGAAC
Jun-B oncogene	AACAGGCAAACAGAAGCCCA	AGATATAAGTAAAACAACTG
Interferon-induced protein with tetratricopeptide	GAAATCAAGGAGATGCTTGA	TGGTAGATAGCCTTGTCTTG
Major histocompatibility complex III	AGGAGAAAAGGAGGGGGCCT	CCCAGCCGTGTCTTCCCAGT
Histocompatibility class II antigen A	GACTCAAATTTCACCCCAGC	TGACTGACTTGCTATTTCTG
Interferon-inducible protein	GGTCCCAGCAGCACAGTGAT	CTTCGTGACTTGTTCCGCTG
Aquaporin 4	GTATGACTAGAGGACAGCAC	TATATCCATTATAGGCTTTT
Chemokine (C-C) receptor 1	AGCCAACAGGTGGACCTGTC	TTTCCACTGTGGATGGGAGG
Matrix metalloproteinase	TGATATCAGCATTTTGGCCC	TACGTTTTCTTCTTCTCCTT
Interferon-gamma	CAGACAGCACTCGAATGTGT	AGGTATACTTTATTCATATG

Discussion

In these studies, we performed gene-profiling analysis in the DSS colitis mouse model using the PPARγ ligand. The upregulated and downregulated genes on PPARγ administration are listed in Table 1. The analysis of the downregulated genes revealed several functional gene clusters with altered expression: (1) oncogene families such as GRO1 oncogenes, (2) inflammatory or immunomediator-related genes such as interferon-gamma, (3) water electrolyte-associated genes, and (4) others.

Furthermore, we identified that the oncogene family genes such as the GRO1, V-maf, and *Jun-B* oncogenes were upregulated in DSS colitis and downregulated in DSS colitis with PPARγ. These oncogenes have been previously reported to be involved in the pathogenesis of IBD;[13,14] therefore further analysis and confirmation is necessary.

Inflammatory mediators such as interferon-γ-related genes[15] or MHC class II genes[16] also have been reported to be involved in IBD pathogenesis. These data are a positive control for this analysis. Water electrolyte-associated genes[17] were not previously known to associate with DSS colitis; therefore, these data should be further corroborated as well. However, it seems very reasonable that these genes are associated with diarrhea, which is the one of the major symptoms of IBD. Among the other genes in Table 2, one interesting gene is the RegIII gene,[18] which is closely related to the regeneration of intestinal epithelium.

Although the initial discrepancy between the data from the high-density oligonucleotide array and the data from quantitative RT-PCR testing was not negligible in this study, the final data presented here were verified by two different methods and should be considered highly reliable. We used real-time quantitative RT-PCR methods for validation of the microarray analysis results. Our validation rate was 60%, which is the same as that previously reported.[12] Gene profiling analysis via the oligonucleotide microarray technique greatly facilitated the study of gene expression in the IBD model mouse treated with PPARγ by showing the global changes in gene expression. Based upon this study, further investigations are now required to identify and confirm the optimal target genes for treating IBD.

Acknowledgments. This study was supported in part by a Yokohama City University Research Grant to A.N., and in part by a grant (SH44211) from the Human Science Foundation to A. N., and also supported in part by a grant (Tokuteiryouiki C #13204072) from the Ministry of Education, Culture, Sports, Science and Technology, Japan, to A.N.

References

1. van Dullemen HM, van Deventer SJ, Hommes DW, Bijl HA, Jansen J, Tytgat GN, Woody J. Treatment of Crohn's disease with

anti-tumor necrosis factor chimeric monoclonal antibody (cA2). Gastroenterology 1995;109:129–35.
2. Lawrance IC, Fiocchi C, Chakravarti S. Ulcerative colitis and Crohn's disease: distinctive gene expression profiles and novel susceptibility candidate genes. Hum Mol Genet 2001;10:445–56.
3. Uthoff SM, Eichenberger MR, Lewis RK, Fox MP, Hamilton CJ, McAuliffe TL, et al. Identification of candidate genes in ulcerative colitis and Crohn's disease using cDNA array technology. Int J Oncol 2001;19:803–10.
4. Dieckgraefe BK, Stenson WF, Korzenik JR, Swanson PE, Harrington CA. Analysis of mucosal gene expression in inflammatory bowel disease by parallel oligonucleotide arrays. Physiol Genomics 2000;4:1–11.
5. Gelman L, Fruchart JC, Auwerx J. An update on the mechanisms of action of the peroxisome proliferator-activated receptors (PPARs) and their roles in inflammation and cancer. Cell Mol Life Sci 1999;55:932.
6. Kersten S, Wahli W. Peroxisome proliferator activated receptor agonists. EXS (Basel) 2000;89:141.
7. Chinetti G, Fruchart JC, Staels B. Peroxisome proliferator-activated receptors (PPARs): nuclear receptors at the crossroads between lipid metabolism and inflammation. Inflamm Res 2000; 49:497.
8. Nakajima A, Wada K, Miki H, Kubota N, Nakajima N, Terauchi Y, et al. Endogenous PPAR gamma mediates anti-inflammatory activity in murine ischemia-reperfusion injury. Gastroenterology 2001;120:460–9.
9. Hippo Y, Taniguchi H, Tsutsumi S, Machida N, Chong JM, Fukayama M, et al. Global gene expression analysis of gastric cancer by oligonucleotide microarrays. Cancer Res 2002;62:233–40.
10. Saubermann LJ, Beck P, De Jong YP, Pitman RS, Ryan MS, Kim HS, et al. Activation of natural killer T cells by alpha-galactosylceramide in the presence of CD1d provides protection against colitis in mice. Gastroenterology 2000;119:11–6.
11. Hippo Y, Yashiro M, Ishii M, Taniguchi H, Tsutsumi S, Hirakawa K, et al. Differential gene expression profiles of scirrhous gastric cancer cells with high metastatic potential to peritoneum or lymph nodes. Cancer Res 2001;61:889–95.
12. Rajeevan MS, Ranamukhaarachchi DG, Vernon SD, Unger ER. Use of real-time quantitative PCR to validate the results of cDNA array and differential display PCR technologies. Methods (Orlando) 2001;25:443–51.
13. Ierardi E, Principi M, Francavilla R, Passaro S, Noviello F, Burattini O, Francavilla A. Epithelial proliferation and ras p21 oncoprotein expression in rectal mucosa of patients with ulcerative colitis. Dig Dis Sci 2001;46:1083–7.
14. Lang SM, Heinzlmann M, Stratakis DF, Teschauer W, Loeschke K. Detection of Ki-*ras* mutations by PCR and differential hybridization and of p53 mutations by SSCP analysis in endoscopically obtained lavage solution from patients with long-standing ulcerative colitis. Am J Gastroenterol 1997;92:2166–70.
15. Bisping G, Lugering N, Lutke-Brintrup S, Pauels HG, Schurmann G, Domschke W, Kucharzik T. Patients with inflammatory bowel disease (IBD) reveal increased induction capacity of intracellular interferon-gamma (IFN-gamma) in peripheral CD8+ lymphocytes co-cultured with intestinal epithelial cells. Clin Exp Immunol 2001;123:15–22.
16. Salomon P, Pizzimenti A, Panja A, Reisman A, Mayer L. The expression and regulation of class II antigens in normal and inflammatory bowel disease peripheral blood monocytes and intestinal epithelium. Autoimmunity 1991;9:141–9.
17. Turtzo LC, Lee MD, Lu M, Smith BL, Copeland NG, Gilbert DJ, et al. Cloning and chromosomal localization of mouse aquaporin 4: exclusion of a candidate mutant phenotype, ataxia. Genomics 1997;41:267–70.
18. Narushima Y, Unno M, Nakagawara K, Mori M, Miyashita H, Suzuki Y, et al. Structure, chromosomal localization and expression of mouse genes encoding type III Reg, RegIII alpha, RegIII beta, RegIII gamma. Gene (Amst) 1997;185:159–68.

Inflammatory Bowel Diseases®
8(5):330–339 © 2002 Crohn's & Colitis Foundation of America, Inc.

Reprinted from INFLAMMATORY BOWEL DISEASES
Vol. 8, No. 5 September 2002
Lippincott Williams & Wilkins Printed in U.S.A.

Peroxisome Proliferator-Activated Receptor Gamma Agonist Ligands Stimulate a Th2 Cytokine Response and Prevent Acute Colitis

*Lawrence J. Saubermann, †Atsushi Nakajima, *‡Koichiro Wada, *Shuping Zhao, §Yasuo Terauchi, §Takashi Kadowaki, ¶Hiroyuki Aburatani, §Nobuyuki Matsuhashi, §Ryozo Nagai, and †Richard S. Blumberg

**Section of Gastroenterology, Boston University Medical Center, Boston; †Gastroenterology Division, Brigham and Women's Hospital, Boston, Massachusetts, U.S.A.; ‡Department of Pharmacology, Osaka University, Osaka; and §Department of Medicine and ¶Genome Science Division, Research Center of Advanced Science and Technology, University of Tokyo, Tokyo, Japan*

Summary: Peroxisome proliferator-activated receptor gamma (PPARγ), a member of a nuclear transcription factor family, has been previously demonstrated to have antiinflammatory activity. The effects of PPARγ activation in the development of an immune response are less well characterized. Through evaluation of PPARγ heterozygote mice ($PPAR\gamma^{+/-}$) and specific PPARγ agonist ligand binding, we evaluated the immunologic effects of PPARγ activation in a well-described model of colitis. Increased susceptibility to dextran sodium sulfate (DSS)-induced colitis as defined by body weights, histologic injury, and survival was observed in the $PPAR\gamma^{+/-}$ mice in comparison to wild-type mice. Three different PPARγ ligands (troglitazone, pioglitazone, and rosiglitazone) demonstrated beneficial dose-related treatment effects when administered prior to the onset of colitis. However, no protection was observed when PPARγ ligand activation occurred after the onset of colitis. The reduction in DSS-induced inflammation noted with PPARγ ligand treatment was associated with decreased interferon-gamma and tumor necrosis factor-alpha and increased interleukin (IL)-4 and IL-10 levels as assessed by quantitative reverse transcriptase-polymerase chain reaction. Consistent with this shift towards a T helper (Th2) cytokine dominance, PPARγ ligand treatment stimulated increased GATA-3 expression. These results indicate that the protective effects exhibited by PPARγ ligands in intestinal inflammation may be due to immune deviation away from Th1 and towards Th2 cytokine production. **Key Words:** Cytokine—T lymphocyte—Transcription factor—Inflammation—Mucosa.

INTRODUCTION

Nuclear transcription factors are key mediators in the induction and maintenance of immune responses, especially in human inflammatory bowel disease (IBD), where activation and translocation of nuclear factor kappa-B (NFκB) complexes may be directly linked to disease pathogenesis (1–7). Recently, another nuclear transcription factor, peroxisome proliferator-activated receptor gamma (PPARγ) (8), has been identified to have important antiinflammatory and immunologic functions (9–11).

Received February 5, 2002; accepted June 3, 2002.

Address correspondence and reprint requests to Dr. L. J. Saubermann, Section of Gastroenterology/Immunobiology Unit, Boston Medical Center, 650 Albany Street, EBRC #507, Boston, MA 02118, U.S.A. E-mail: lawrence.saubermann@bmc.org

Peroxisome proliferator-activated receptor gamma (PPARγ) is highly conserved between species (12,13), and is expressed at increased levels in the colon, and to a lesser extent the small intestine, of rodents and humans (8,14–17). Upon activation, PPARγ binds in a heterodimeric fashion with retinol X receptor-α (RXRα) to peroxisome proliferator responsive elements (PPREs) that are present on a number of gene promoter regions (18–20). Many of these PPREs are found on promoters associated with proinflammatory cytokines, such as tumor necrosis factor-alpha (TNFα) and interleukin-1 (IL-1), which are inhibited by PPARγ. In addition to directly regulating cytokine production, PPARγ agonists may indirectly affect proinflammatory genes by inhibiting the function of other nuclear transcription factors such as AP-1 and the NFκB complex (21,22). These antiinflammatory effects of PPARγ indicate that it may play a very

important role in reducing tissue inflammation associated with innate and adaptive immune responses. Indeed, PPARγ agonists have demonstrated significant innate antiinflammatory effects. For instance, PPARγ significantly reduces NO activity via reduction of iNOS, and potentially has direct effects on NO itself (23–28). In addition; many inducible inflammatory chemokines such as IL-8 (29,30), MCP-1 (31), IP-10, MIG, and I-TAC (32), which influence the tissue migration of many types of leukocytes, are significantly inhibited by PPARγ activation.

PPARγ activation also appears directly to influence the development of an adaptive immune response. The production and release of IL-12 by macrophages/dendritic cells is critical to the development of a CD4+ T helper 1 (Th1) response (33), which appears to be the dominant response observed with Crohn's disease. PPARγ has been demonstrated to reduce IL-12 production directly through inhibition of IL-12 messenger RNA levels (34). In addition, PPARγ inhibits the release of IL-2 by Th1 CD4+ lymphocytes (35,36), apparently through direct interactions with the nuclear transcription factor NFAT (36). PPARγ also may exert selective influences on Th1 lymphocytes by an increase in apoptosis, as has been observed in peripheral blood lymphocytes of mice (37). By these varied mechanisms, PPARγ could potentially influence the development of a Th1 adaptive cellular response in vivo.

In vivo animal studies have indicated that PPARγ activation leads to a reduction in Th1-associated transcription factors, cytokines and chemokines, resulting in decreased intestinal inflammation associated with administration of dextran sodium sulfate (DSS) or the hapten trinitrobenzene sulfonic acid (TNBS) (29,30,38). However, these investigations did not directly address whether PPARγ affected the development of a Th1 immune response relative to a Th2 response.

In this article, we investigated the in vivo role of PPARγ in the induction of colitis associated with a Th1 cytokine excess. We therefore studied the acute DSS colitis model, which is known to be dependent on Th1-associated cytokines for its development. In this model, we investigated PPARγ$^{+/-}$ mice and the therapeutic response to three different PPARγ ligands in the development of colitis. Furthermore, we examined the pretreatment response compared with posttreatment response for the most effective of these ligands. These investigations strongly support an important role for PPARγ as an endogenous antiinflammatory mediator. Moreover, we observed that PPARγ ligands introduced prior to the onset of, but not after, acute DSS colitis could provide antiinflammatory protection and do so by shifting the cytokine balance and transcriptional regulation of T cells away from Th1 and towards a Th2 predominance.

MATERIALS AND METHODS

Mice

Inbred C57BL/6 mice were purchased from Jackson Laboratories (Bar Harbor, ME, U.S.A.). The PPARγ$^{+/-}$ (heterozygotic) mice were generated as previously described (30). All animals were maintained under specific pathogen-free conditions on standard laboratory chow and water ad libitum until the desired age (7–10 weeks) and/or weight (20–30 gm) were achieved. All mice were treated humanely according to National Institutes of Health, IACUC, and the Panel on Euthanasia of the American Veterinary Medical Association guidelines.

Dextran Sodium Sulfate (DSS) Colitis Model

Dextran sodium sulfate (Lot 7359c; ICN, Aurora, OH, U.S.A.) was added to the animals' water supply at a concentration of 2.5% (wt/vol) at Day 0 of each experiment and animals were allowed to drink freely. Total body weight (g) was measured at the same time each day and prior to introduction of the PPARγ ligand by gavage. Feces were collected from each mouse daily and stored for rehydration and fecal occult bleeding measurements. For analysis of fecal occult bleeding, daily stools were resuspended in 400 μl of sterile water through vortexing for 5 min, microcentrifuged at 13,000 rpm for 2 min using an Eppendorf 5417C table-top centrifuge (Hamburg, Germany), and then 40 μl of supernatant was added to paper from the Hemoccult SENSA (SmithKline Diagnostics, San Jose, CA, U.S.A.) kit. Scoring for diarrhea (0–3) and fecal blood (0–4) were performed as previously reported (39). Daily gavage of the PPARγ ligands began on Day −1 in all the experiments, except for one experiment where it was begun on Day +1 (see Results). All experiments were repeated at least twice with 5 to 10 mice per group. The data displayed provides a summary of the results.

Reagents

Troglitazone was obtained from Parke-Davis (Morris Plains, NJ, U.S.A.), rosiglitazone (BRL-49653) from SmithKline Beecham (Tokyo, Japan), and pioglitazone from the Sato Chemical Corporation (Japan). Other reagents were of chemical grade.

Histologic Staining

For histologic staining, tissue samples were fixed in 3.7% formaldehyde-PBS overnight at 4°C. The samples were then dehydrated and embedded in paraffin. Three-micrometer sections were stained with hematoxylin and eosin (HE).

Western Blot Analysis for GATA-3 Expression

Tissue samples were collected from animals that had received DSS for 1 week in the presence or absence of rosiglitazone (30 mg/kg per day). The samples were homogenized in Tris-HCl buffer with a cocktail of protease inhibitors and then centrifuged. Supernatants were subjected to SDS-PAGE electrophoresis (30 μg protein per sample per lane). Expression of GATA-3 in tissues was detected using a GATA-3-specific polyclonal antibody (Santa Cruz Biotech, Santa Cruz, CA, U.S.A.). The Vectastain ABC kit (Vector Laboratories, Burlingame, CA, U.S.A.) was used with 3,3′-diaminobenzidine (DAB) substrate kit (Vector Laboratories) according to the manufacturer's instructions for detection.

Cytokine Analysis

Quantitative polymerase chain reaction (PCR) was performed for cytokine measurements using cDNA samples derived through reverse transcription (RT)-PCR of whole colon mRNA. mRNA was isolated using the RNAeasy kit (Qiagen, Germany), followed by performance of RT-PCR using MMLV as previously described (30). cDNA amounts and purity were checked by spectrophotometry using the DU-640 spectrophotometer at wavelengths 260 and 280. cDNA samples were then used as templates for individual PCR reactions using specific primer sets for TNFα, IL-4, IL-10, and interferon-gamma (IFNγ). The quantitative PCR analysis was performed using ABI 7700 real-time PCR machine (Taq-Man). The specific primers for IL-10, IL-4, IFNγ, and TNFα were purchased from ABI.

Statistical Analysis

All results are expressed as mean ± SEM. Statistical comparisons were made using the Student *t* test after the analysis of variances. The results were considered significantly different at $p < 0.05$.

RESULTS

Mice That Are Heterozygotic for PPARγ Expression Demonstrate Increased Susceptibility to DSS-Induced Colitis

Since agonism of PPARγ has been previously demonstrated to have a beneficial effect on DSS-induced colitis in vivo (29), it is predicted that a lack of PPARγ would result in a worsening of colitis. To explore this possibility, we initially tested mice that were heterozygotic for PPARγ expression ($PPAR\gamma^{+/-}$) in the DSS colitis model and compared their response to wild-type control animals. $PPAR\gamma^{+/-}$ mice were used in these experiments, as homozygotic mice do not survive for very long after parturition. Although they express significantly diminished quantities of PPARγ, $PPAR\gamma^{+/-}$ mice otherwise appear normal in morphologic analysis (30). After receiving 7 days of DSS treatment, $PPAR\gamma^{+/-}$ mice exhibited significantly greater mortality in comparison to DSS treated wild-type control animals of the same genetic background and under similar environmental conditions (Fig. 1A). Typical of DSS-induced colitis, diarrhea and grossly bloody feces were clearly evident in the treatment groups, while untreated $PPAR\gamma^{+/-}$ littermates were otherwise clinically normal (data not shown). In conjunction with the observation on mortality, there was a corresponding exacerbation of weight loss (Fig. 1B) and loss of mucosal epithelium and enhanced ulceration (Fig. 1C) in the DSS-treated $PPAR\gamma^{+/-}$ mice in comparison with the wild-type control mice. These results emphasize the increased susceptibility of the $PPAR\gamma^{+/-}$ mice to the development of colitis induced by DSS administration, as we have previously observed in response to ischemia-reperfusion injury (30). They further emphasize the importance of endogenous PPARγ in regulating the degree of tissue inflammation associated with pathologic injuries and provide physiologic relevance to previous studies with this model (29).

Dose Responses Differ for Three PPARγ Agonist Ligands

Previous studies have also shown the therapeutic effects of PPARγ agonists in the chronic DSS model (29). In the next series of experiments we sought to confirm and extend these observations in the acute DSS colitis model by examining three different thiazolidinediones (TZDs): troglitazone, rosiglitazone (BRL-49653), and pioglitazone. Using DSS-susceptible C57BL/6J mice, the dose response for each of the PPARγ ligands was evaluated and compared with untreated control animals that received DSS alone. All three TZDs provided clinical protection against colitis as defined by body weight with varying dose responses when administered at Day −1 of exposure to DSS (Fig. 2A).

Identical observations were made when diarrhea and occult bleeding were assessed (data not shown). Specifically, pioglitazone and rosiglitazone resulted in significantly less colitis at relatively equivalent dose ranges in

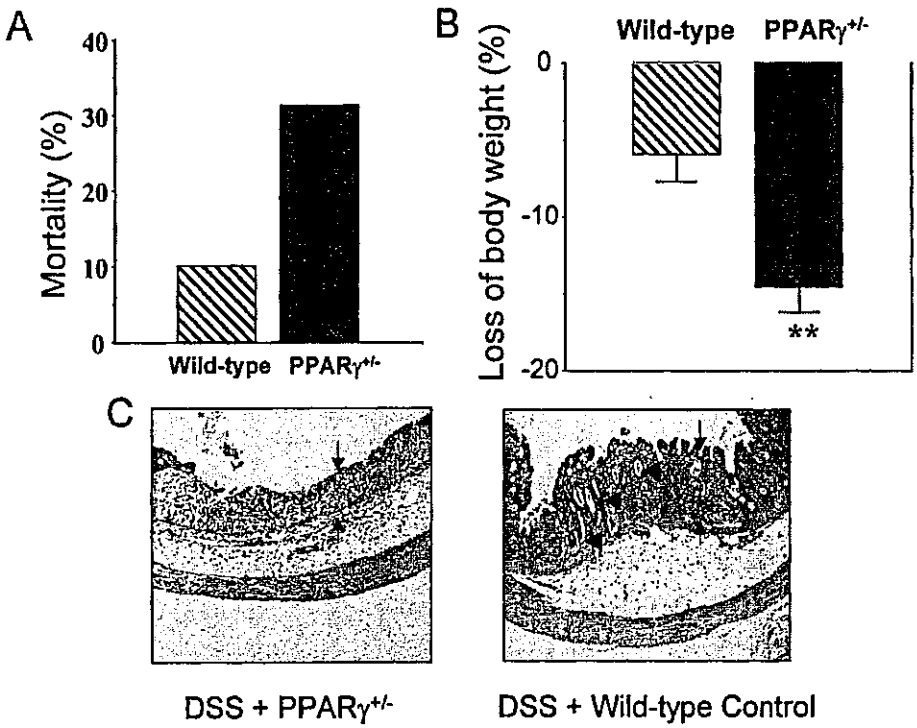

FIG. 1. Reduction in endogenous PPARγ is associated with an increased susceptibility to DSS-induced colitis. **A:** The mortality percentage was significantly higher in DSS-treated PPARγ heterozygote (PPARγ$^{+/-}$) mice as compared with DSS-treated wild-type control mice. Mice were treated for 1 week with 2.5% DSS given ad libitum in their drinking water. Both groups consumed equal amounts of DSS-treated water. **B:** Dally weights were determined for the same group of animals as in Panel A, and the percentage loss in body weight from baseline after 1 week is shown. There was a significant difference in the loss of body weight between the two groups (**, $p < 0.01$). **C:** Histologic appearance of PPARγ$^{+/-}$ mouse colon tissue (**left panel**) as compared with wild-type control mouse colon tissue (**right panel**) receiving 2.5% DSS for 1 week. As shown in these representative samples, PPARγ$^{+/-}$ mice had a much greater inflammatory infiltrate with loss of the mucosal surface (arrows). Colonic crypts (arrowheads) are still evident in the wild-type control mouse sample, yet are not seen in the PPARγ$^{+/-}$ mouse tissue. Hematoxylin and eosin stained sections are shown at similar magnifications.

comparison with troglitazone, which was demonstrably less effective. It should be noted that at the maximum dose for troglitazone (200 mg/kg) it was difficult to maintain solubility. Both pioglitazone and rosiglitazone appeared to achieve a significant therapeutic effect with a daily dosage of 10 mg/kg, which reached a plateau by the higher dosage of 30 mg/kg. Rosiglitazone appeared to have a slightly better effect at 10 mg/kg than piog-

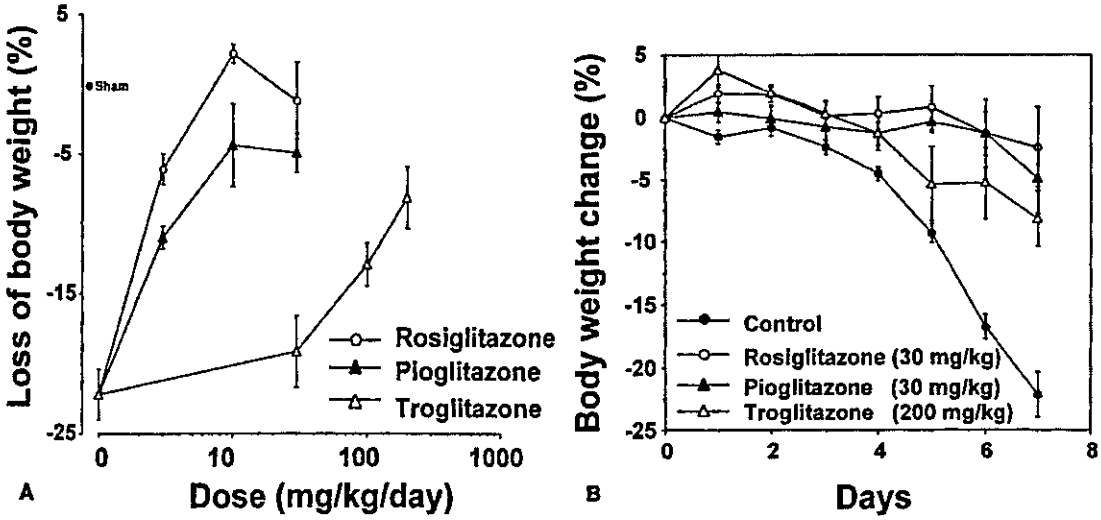

FIG. 2. Dose response curves (**A**) and preventative effects (**B**) for three PPARγ agonist ligands (troglitazone, rosiglitazone [BRL-49653], and pioglitazone) or control vehicle. Each ligand or control was introduced by gavage to C57BL/6 mice 1 day before administration of 2.5% DSS in their drinking water. Measurement of body weight, as a percentage of starting weight, is shown. Body weight changes corresponded to occult fecal bleeding and degree of diarrhea (data not shown). No differences between groups in their intake of DSS were noted.

litazone, but this advantage was lost by the 30 mg/kg dosage. These studies confirm the previously observed beneficial effects of BRL-49653 on experimental DSS-induced colitis (29), and show that these effects likely extend to the whole TZD class of compounds with varying efficacy.

Varying Effects of Treatment Regimens with PPARγ Ligands on DSS Colitis

Our previous studies with PPARγ-deficient animals suggested the importance of endogenous PPARγ activity in protecting from colitis in an ischemia-reperfusion injury model (30). It was important therefore to determine whether the beneficial activity of PPARγ activation was occurring during the early and/or later phases of colitis. To define this, we compared the effects of PPARγ ligands administered before and after colitis induction. In the former case, each ligand was begun at Day −1 in the DSS colitis model. As demonstrated in Figure 2A, there was significantly less weight loss in all of the TZD treatment groups in comparison with the untreated control animals when administered prior to exposure to DSS. As described above, rosiglitazone and pioglitazone were significantly better than troglitazone. These findings were confirmed by microscopic histologic examination (Fig. 3).

In a second series of studies, the antiinflammatory effects of administering the PPARγ agonist ligands after the onset of acute DSS-induced colitis were evaluated. Two groups of C57BL/6J mice received either rosiglitazone 30 mg/kg or control vehicle by gavage beginning on Day +1 of DSS administration. Unlike the pretreatment regimen described above, there were no demonstrable differences in weight loss or any of the other measured parameters observed between the two groups (Fig. 4). These findings indicate that PPARγ may play a preventive, rather than a therapeutic, role in the acute DSS-induced colitis model. They further emphasize the importance of endogenous PPARγ activity as described above, and imply an important and perhaps essential role for PPARγ during the earliest phases of tissue inflammation.

PPARγ Ligands Down-Regulate Th1 and Up-Regulate Th2 Cytokine Production in Acute DSS Colitis

Since it has been shown that PPARγ can result in a change in the immunologic function of many different

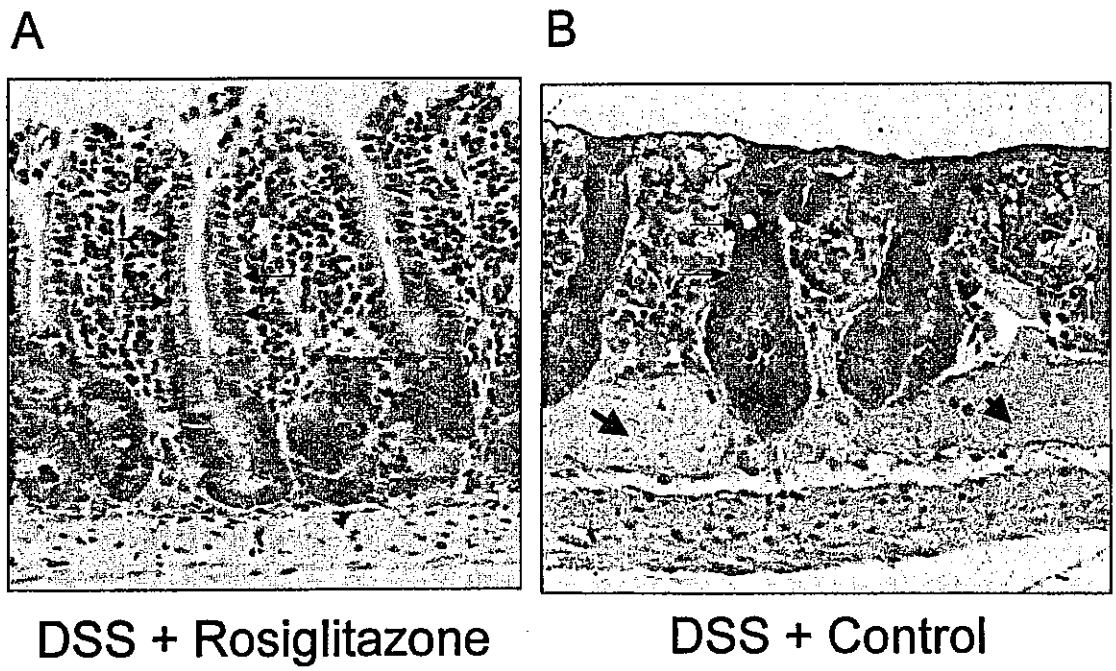

FIG. 3. Histologic appearance of DSS-treated C57BL/6 mouse colon tissue confirms protective effect of PPARγ-ligand activation. Inbred C57BL/6 mice received either rosiglitazone (**A**) or control vehicle (**B**) by daily gavage 1 day prior to initiating 2.5% DSS-induced colitis. There was notable preservation of the colonic crypt epithelium in the rosiglitazone-treated tissue sample (thin arrows), as compared with the control treated tissue. There also was increased submucosal hemorrhage (thick arrows) in the control-treated tissue sample that was not present in the rosiglitazone-treated sample. Representative hematoxylin and eosin stained sections from day 4 are presented at similar magnifications.

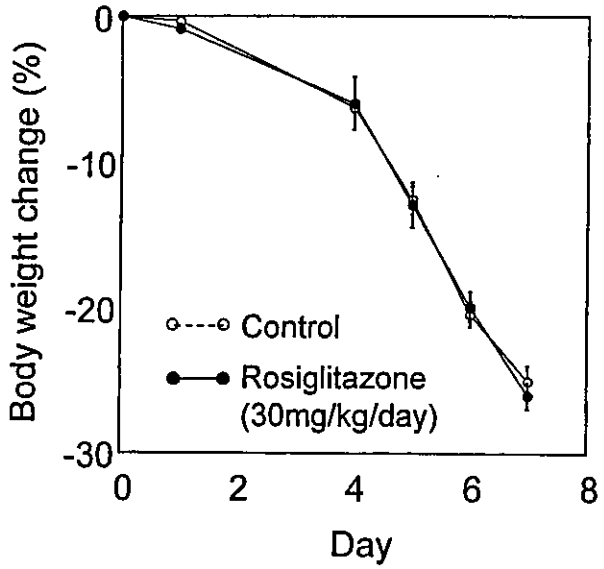

FIG. 4. Ineffectiveness of PPARγ ligand, rosiglitazone, at reducing acute DSS-induced murine colitis in a therapeutic treatment trial. Two groups of inbred C57BL/6 mice received rosiglitazone, or control vehicle, by daily gavage beginning 24 hours after the onset of 2.5% DSS-induced colitis. Measurements of body weights, as a percentage of initial weights, are shown. These body weight changes corresponded to occult fecal hemorrhage and degree of diarrhea (data not shown). There were no noted differences between groups in their intake of DSS.

cell types, including macrophages and T cells, we sought to understand the effects of the TZD class of PPARγ ligands on cytokine production in the context of DSS-induced tissue inflammation. Quantitative PCR for tissue-associated cytokines was performed from cDNA prepared from samples generated from whole colon on Day +4 of the DSS colitis model using rosiglitazone (10 mg/kg/day) as the PPARγ agonist when administered at Day −1 of DSS administration. Marked differences in the levels of IL-10, IL-4, IFNγ, and TNFα were observed in the ligand-treated mice in comparison with the untreated mice. Specifically, rosiglitazone induced an increase in IL-10 and IL-4 levels, and a reduction in IFNγ and TNFα levels, consistent with a shift towards a Th2 cytokine bias (Fig. 5). These data suggest that the beneficial effects of the TZD class of agents in the DSS colitis model is not simply due to a reduction in Th1 cytokine production normally associated with this model, but that it also is due to a concurrent increase in Th2 cytokine production.

Colonic GATA-3 Expression Is Consistent With Th2 Cytokine Predominance

Since expression of the nuclear transcription factor GATA-3 plays a major role in the development of a Th2 response (33), we sought to evaluate the possibility that PPARγ ligand-induced activation was associated with up-regulation of GATA-3 expression. As shown in Figure 6, there was a significant elevation in the quantities of GATA-3 detectable in the rosiglitazone-treated animals in comparison with wild-type, untreated controls. These results are consistent with the observed increase in Th2 cytokines at the transcriptional level and the possible deviation of the Th immune response induced by PPARγ activation.

DISCUSSION

In this article, we have confirmed that PPARγ ligands are effective at influencing the development of an immune response by reducing Th1-associated cytokines

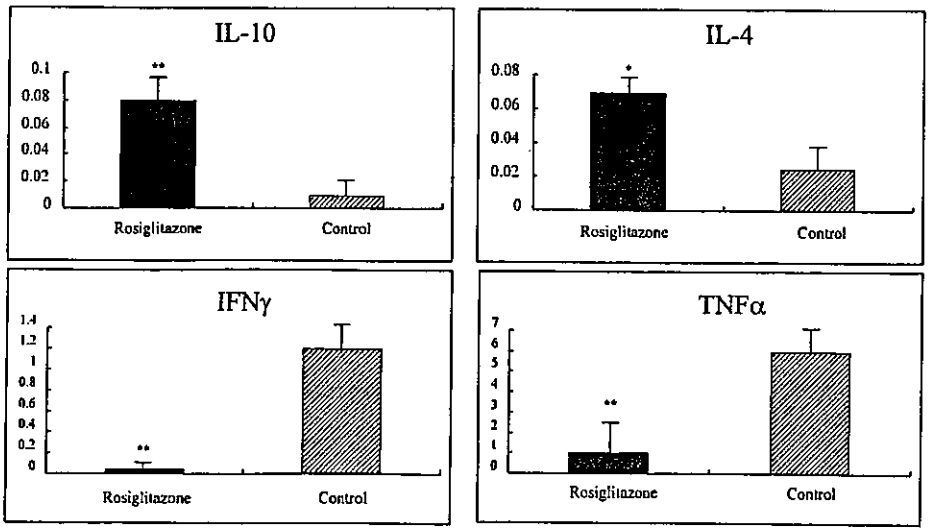

FIG. 5. Quantitative reverse transcriptase-polymerase chain reaction cytokine analysis. PPARγ ligand, rosiglitazone (10 mg/kg), or control vehicle was administered to C57BL/6 mice by daily gavage 1 day prior to treatment with 2.5% DSS. Quantitative cytokine measurements were performed for TNFα and Interferon-gamma (IFNγ) (Th1 cytokines), and IL-10 and IL-4 (Th2 cytokines), from whole colon samples on Day 4 of DSS treatment. Preadministration of PPARγ ligand, rosiglitazone, in DSS-induced colitis resulted in significant reductions in Th1 cytokines and increases in Th2 cytokines, as compared with control treated animals (*, $p < 0.05$; **, $p<0.01$).